

A NEW EXPERIMENTAL STATION FOR LIQUID INTERFACE X-RAY SCATTERING AT NSLS-II BEAMLINE 12-ID

D. M. Bacescu[†], L. E. Berman, S. L. Hulbert, B. M. Ocko, Z. Yin, National Synchrotron Light Source II (NSLS-II), Brookhaven National Laboratory, Upton, New York 11973, USA

Abstract

Open Platform and Liquids Scattering (OPLS) is a new experimental station recently built and currently being commissioned at the Soft Matter Interfaces (SMI) beamline 12-ID at NSLS-II. The new instrument expands SMI's beamline scientific capabilities via the addition of X-ray scattering techniques from liquid surfaces and for measurements that require an open platform.

The design of this new instrument, located inside the 12-ID-B beamline shielding enclosure, uses a single Ge (111) crystal deflector to bounce the incident x-ray beam by a variable angle α downwards away from the horizontal by rotating the large Huber Eulerian cradle χ stage. Tilting the beam is essential for liquid samples where gravity dictates the sample normal.

The OPLS instrument has a variable deflector-to-sample distance ranging from 0.6 m to 1.5 m where the larger distances are preferred for large processing chambers. Up to three X-ray detectors are mounted on a 2-theta scattering arm located downstream of the sample location. These detectors support a variety of X-ray techniques including X-ray reflectivity (XR), Grazing Incidence (GI) Small-Angle X-ray Scattering (SAXS) and Wide-Angle X-ray Scattering (WAXS), and grazing-incidence angle X-ray fluorescence.

Currently, the OPLS experimental station intercepts the 12-ID beam that otherwise propagates to the SMI experimental station located in hutch 12-ID-C and can be retracted to a "parking" position laterally out of this beam to allow installation of a removable shielded beam pipe that is needed to support operations in hutch 12-ID-C.

The design of OPLS is flexible enough to adapt to a planned future configuration of the SMI beamline in which OPLS is illuminated independently of SMI via a second, canted undulator source and a separate photon delivery system. In this future configuration, both branches will be able to operate independently and simultaneously.

INTRODUCTION

SMI beamline is one of the five beamlines of the Complex Scattering Program at NSLS-II. The beamline is served by a 2.8m long, 23mm period length, in-vacuum undulator (IVU23) generating x-rays with energy ranging from 2.05 – 24 keV. OPLS, one of the two experimental stations of the 12-ID (SMI) beamline, is located at approx. 51m from the source, inside shielded hutch enclosure, 12-ID-B (see Fig. 1). The OPLS uses the same photon delivery system as the SMI branch. The bimorph optical mirrors of

the SMI beamline can focus the beam at one of the two end station or at a secondary source aperture.

The OPLS experimental station is a liquid surface spectrometer designed with an open sample platform, which is a unique feature which offers high versatility, and allows X-ray scattering studies from liquid surfaces and interfaces, as well from different processing environments (e.g., roll-to-roll processing). The OPLS experimental station is designed to operate from 8 – 24 keV, with a beam spot size of approx. 20 μm vertically and 400 μm horizontally, and a photon flux of approx. 10^{12} ph./sec. [1].

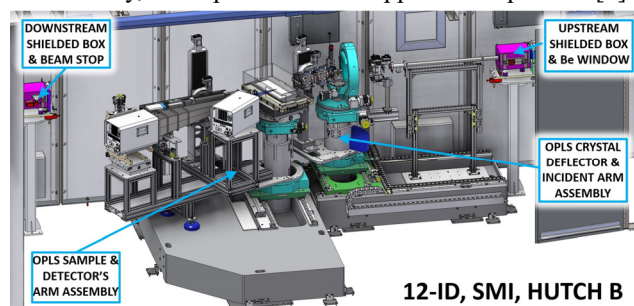


Figure 1: OPLS instrument (shown in operation mode).

THE OPLS DESIGN OVERVIEW

To illuminate the rear hutch (12-ID-C) the SMI X-ray beam propagates through a removable and interlocked shielded beam transport pipe (approx. 4.5 m long), located in hutch 12-ID-B. For OPLS operation, this beam pipe is removed, the upstream vacuum section is terminated by a Beryllium (Be) window and a removable lead beam stop is mounted at the downstream end, thereby defining the space available for OPLS experimental station.

The Crystal Deflector Assembly

The crystal deflector assembly (see Fig. 2) has a granite base (0.89m×1.85m×0.30m) with sufficient length to allow the motion along Z-axis, to accommodate a variable deflector-to-sample distance ranging from 0.6 m to 1.5 m.

The Z-axis translation stage ($\pm 650\text{mm}$) is actuated by a stepper motor and rack and pinion mechanism. To overcome the pinion backlash, the motion control system uses feedback from an incremental encoder. To lock the stage into position, an air-actuated clutch-brake module is used on the inboard guide rail. The brake module uses spring energy to clamp onto the guide rail and air pressure to overcome the spring force and release it [2].

The X-axis translation stage ($\pm 150\text{mm}$), actuated by a stepper motor and a preloaded ball screw assembly (NSK PSS25-05-N1-D-0499), is used to center the crystal deflector into the beam using the cross-hair alignment

[†] dbacescu@bnl.gov

target, or to move it out of the beam, to the retracted position, when OPLS is not operated. Both Z and X axes translation stages are based on pairs of linear roller guides (NSK RA30 series), incremental encoders and limit switches.

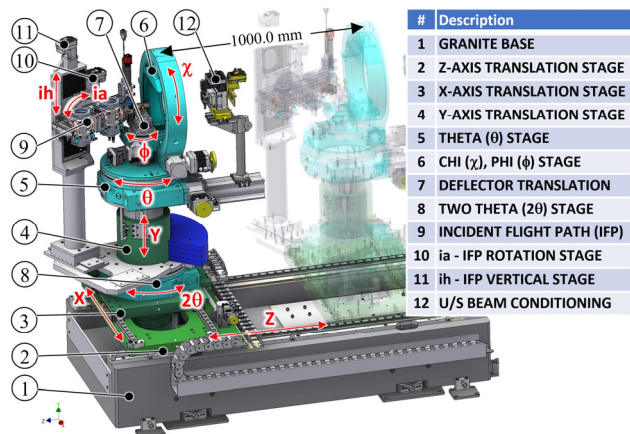


Figure 2: Deflector crystal and incident arm assemblies.

The Y-axis vertical stage with vertical stroke of ± 75 mm, is a recycled component from a former instrument. It consists of two concentric and guided cylinders and is actuated by motorized a screw jack assembly. Mounted on top of the Y-axis translation stage is a 3-circle goniometer consisting of a θ -stage (Huber 430) and an Eulerian cradle (Huber 512.1). The θ -stage is used to position the χ -stage perpendicular to the incoming beam. The χ -stage is used to rotate the crystal and bounce the incident X-ray beam downwards by a variable angle α from horizontal. The ϕ -stage is used to set the Bragg angle [3]. Above the ϕ -stage, there is an additional crystal translation stage which positions the crystal or a cross-hair alignment target at the Eulerian cradle's center. On top of the X-axis translation stage, a 2θ -stage (Huber 430) provides rotation of the incident arm. The arm is holding a vertical ih-translation stage (Daedal 406004LN) on which the ia-goniometer (Huber 411) is mounted, where the ia-rotation axis orientation is horizontal. All these motions allow the alignment of the incident flight path with the deflecting beam angle α . A beam conditioning module is located upstream of the χ -stage, attached to the base θ -stage, consisting of an absorber bar, beam slits, photon shutter, and an ion chamber (see Fig. 2).

The Incident Flight Path (IFP)

The compact incident flight path was designed to fit within the specified minimum deflector-to-sample distance. All components of the IFP are mounted on an extruded aluminum rail. The IFP (see Fig. 3) consists of a vacuum section with in-vacuum slits centered on the ia-axis and vacuum crosses at the upstream and downstream ends, each equipped with end flanges holding Kapton® windows. Also, ion chambers are attached at each end of the vacuum section. The upstream vacuum cross house a vertically retractable Diamond Beam Position Monitor (DBPM) and a filter selector (see Fig. 3b).

The downstream vacuum cross is used for pumping and can house an optional secondary DBPM. A beam visualization module is located upstream of the IFP (see Fig. 3c), consisting of a 100 μ m thick Cadmium Tungstate (CdWO₄) polished crystal scintillator plate, a 30 mm cage cube-mounted silver-coated turning mirror, a 5X Mitutoyo objective lens, a 152.5mm-long extension tube, and a CMOS monochrome camera (Allied Vision Mako G-419B). An in-air attenuator translator bar is mounted downstream of the IFP, (see Fig. 3a).

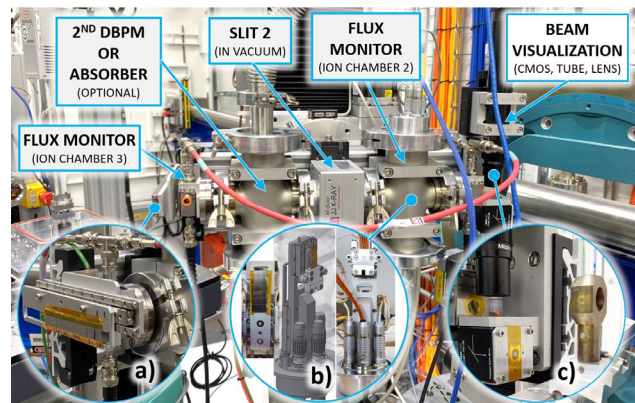


Figure 3: Incident flight path assembly. a) in-air attenuator translator bar; b) DBPM & absorber; c) beam visualization scintillator, mirror, and objective lens.

The Sample and Detector Arm Assemblies

The sample and detector arm assemblies (see Fig. 4) are mounted on a granite base (1.62m \times 2.43m \times 0.30m) with sufficient length and width to allow the sample assembly, together with the detector arms, to translate along the X-axis. In addition, the detector arms are rotated by the 2θ -stage (Huber 440) about an axis concentric with sample vertical translation.

The geometry code translates in X-axis and Y-axis so that the downward deflected beam intercepts the center of the sample. The detector arms are supported by a pair of flat and round air bearings that ride on the top surface of the granite base and can rotate from $2\theta=0^\circ$ position (parallel with Z-axis) to $2\theta=90^\circ$ (perpendicular to Z-axis) for any X-axis position in operation mode.

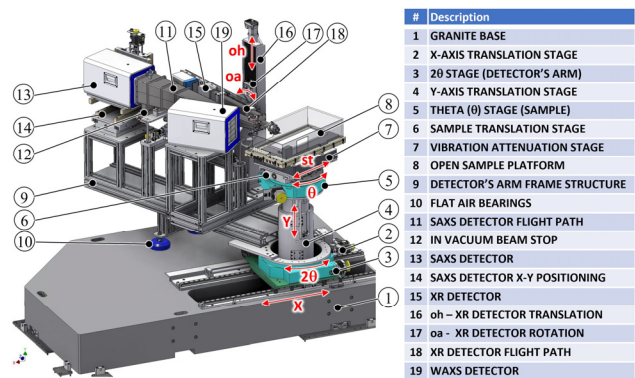


Figure 4: The OPLS sample and detector arm assemblies.

The detectors arms are constructed from extruded aluminum structural framing, designed to hold up to three

detectors located downstream of the sample, with fixed 20° angular offsets, each dedicated to a different technique.

The XR detector assembly is supported on the inboard side of the detector's frame structure, with 11° inboard angular offset. The XR detector uses a Lambda 250k GaAs detector (55 μm pixel size) interchangeable with a Dectris Pilatus 100K detector. The XR detector is located 1.0 m downstream from the sample, mounted downstream of a rectangular cross-section flight tube. Both detectors are mounted on extruded aluminum rail which can be rotated horizontally by the ϕ -axis stage (Huber 411) and translated vertically by the z -axis stage. All these motions allow the XR detector to be positioned at an angle β with respect to the horizontal whose height is arranged to intercept the reflected beam from the sample.

The SAXS detector assembly (see Fig. 5) consists of a detector flight path and is equipped with an in-vacuum beam stop (with x and y translations, see Fig. 5b) and a flight path motion system. The flight path motion system is based on two custom-designed vertical translation stages, located at the end, each actuated by a motorized screw jack. The downstream end has a hinge that is coupled with the corresponding vertical translation stage (Fig. 5c).

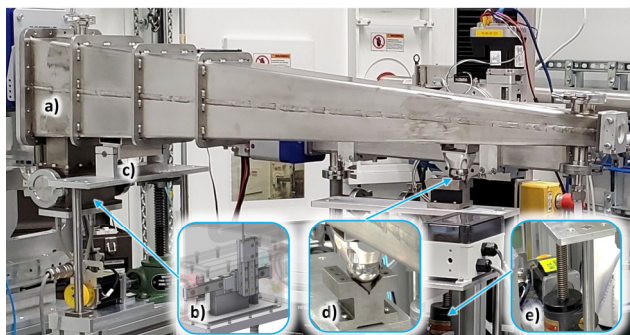


Figure 5: The SAXS detector flight path assembly. a) Flight path; b) in-vacuum beam stop; c) hinge; d) upstream pivot; e) upstream vertical stage.

The upstream end has a spherical pivot which sits on a “V” groove (Fig. 5d) located above the upstream vertical stage. By moving the two vertical stages, the flight path can be adjusted in height or inclined (moving differentially, with the downstream end higher than upstream one) around a virtual axis located at the sample position. The current setup locates the SAXS detector at 1.5m from the sample. The detector is not coupled to the flight path and can be positioned by a set of X-Y custom-made translation stage modules. The setup is compatible with either a Dectris Pilatus 300K or 1M detectors. The WAXS detector is supported on the outboard side of the on same frame structure, with 20° outboard angular offset and at a distance between 0.3-0.5 m from the sample. The WAXS detector is designed for a Dectris Pilatus 1M.

The sample positioning mechanism design is similar to the one described for the crystal deflector assembly except that there is no Z-axis translation (not required). The sample X-axis translation stage has stroke of ±435mm and the sample Y-axis vertical stage has a stroke of ±125mm. The sample rotates using a θ -stage (Huber 430) on top of

which there is a custom-made sample translation stage (stroke ±180mm). An active vibration isolation table (Herzan TS-150), mounted on top of the sample translation stage, can support a maximum load of 150 kg and maximizes the instrument resolution by removing the ambient vibration noise (less than 5 Hz).

Commissioning Results

This Fig. 6 shows the ϕ rocking scan profiles at 16.1 keV, for various downward projected angles α from 0° to 4° deg. The rocking curve width are dominated by the Ge (111) deflection crystal's Darwin width. The deviation in the centroid of these rocking curves varies by about +/- 0.0002°, more than adequate for a single χ motion to deflect the beam downwards and much less than the Darwin width.

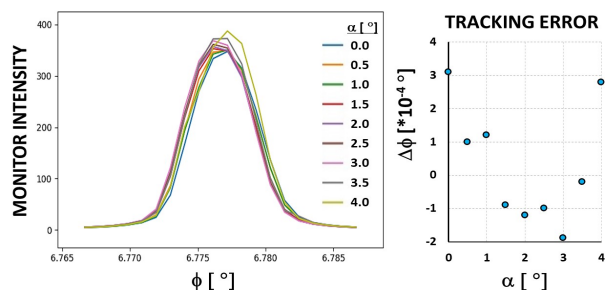


Figure 6: Instrument tracking @ 16.1 keV.

CONCLUSIONS

The OPLS is fully assembled and functional. The experimental station was recently successfully commissioned, and soon will start the general user operation.

ACKNOWLEDGEMENTS

The authors would like to extend their gratitude to the entire beamline support team, especially to Rick Greene and Leo Reffi for their technical support and Chris Stebbins for his project coordination. The Work was supported by the National Synchrotron Light Source II, a U.S. Department of Energy (DOE) Office of Science User Facility operated for the DOE Office of Science by Brookhaven National Laboratory under Contract No. DE-SC0012704.

REFERENCES

- [1] Mikhail Zhernenkov, Niccolo Canestrari, Oleg Chubar, Elaine DiMasi, “Soft matter interfaces beamline at NSLS-II: geometrical ray-tracing vs. wavefront propagation simulations,” in *Advances in Computational Methods for X-Ray Optics III, Proc. SPIE*, vol. 9209, p. 92090G, 2014.
- [2] Nexen Group, <https://www.nexengroup.com/>
- [3] Peter S. Pershan, Mark Schlossman, *Liquid Surfaces and Interfaces: Synchrotron X-Ray Methods*. Cambridge: Cambridge University Press, 2012